Geophysical Research Letters

Key Points:

- We investigate structure and seismicity at the updip end of the 2014 Iquique earthquake rupture using amphibious seismic data
- Seismicity updip of the 2014 Iquique earthquake occurs over a broad range likely interpreted to be related to the basal erosion processes
- Coseismic stress changes and aftershocks activate extensional faulting of the upper plate and subduction erosion

Correspondence to:

F. Petersen,
flpetersen@geomar.de

Relationship Between Subduction Erosion and the Up-Dip Limit of the 2014 Mw 8.1 Iquique Earthquake

Florian Petersen[1] ![ORCID], **Dietrich Lange**[1] ![ORCID], **Bo Ma**[1] ![ORCID], **Ingo Grevemeyer**[1] ![ORCID], **Jacob Geersen**[2] ![ORCID], **Dirk Klaeschen**[1] ![ORCID], **Eduardo Contreras-Reyes**[3] ![ORCID], **Sergio Barrientos**[4], **Anne M. Tréhu**[5] ![ORCID], **Emilio Vera**[3] ![ORCID], **and Heidrun Kopp**[1,2] ![ORCID]

[1]GEOMAR Helmholtz Centre for Ocean Research Kiel, Kiel, Germany, [2]Institute of Geosciences, Kiel University, Kiel, Germany, [3]Departamento de Geofísica, Facultad de Ciencias Físicas y Matemáticas, Universidad de Chile, Santiago, Chile, [4]Centro Sismológico Nacional, Facultad de Ciencias Físicas y Matemáticas, Universidad de Chile, Santiago, Chile, [5]Oregon State University, College of Earth, Ocean, and Atmospheric Sciences, Corvallis, USA

Abstract The aftershock distribution of the 2014 Mw 8.1 Iquique earthquake offshore northern Chile, identified from a long-term deployment of ocean bottom seismometers installed eight months after the mainshock, in conjunction with seismic reflection imaging, provides insights into the processes regulating the updip limit of coseismic rupture propagation. Aftershocks updip of the mainshock hypocenter frequently occur in the upper plate and are associated with normal faults identified from seismic reflection data. We propose that aftershock seismicity near the plate boundary documents subduction erosion that removes mass from the base of the wedge and results in normal faulting in the upper plate. The combination of very little or no sediment accretion and subduction erosion over millions of years has resulted in a very weak and aseismic frontal wedge. Our observations thus link the shallow subduction zone seismicity to subduction erosion processes that control the evolution of the overriding plate.

Plain Language Summary To better understand the controls on shallow seismicity and subduction erosion following large subduction earthquakes, we use marine recordings of the Mw 8.1 2014 Iquique earthquake aftershocks and long-offset multi-channel seismic data. By comparing the aftershock locations and seismic imaging, we observe that most aftershocks occurred in the upper continental plate and abruptly stopped in the frontal forearc. The amplitude characteristics of upper-crust reflections indicate a fractured and fluid-filled outer forearc, which is associated with the absence of aftershocks. Large-scale faulting, as evidenced by disrupted reflections in the seismic image, can be correlated to upper plate seismicity. We propose that the aftershocks updip of the main earthquake area reflect active subduction erosion processes.

1. Introduction

The largest earthquakes on the globe occur along convergent plate margins, rupturing the boundary between upper overriding and lower subducting plates. For most subduction zones, the precise location of the far offshore located updip limit of coseismic slip and its controlling parameters remain poorly resolved, despite being of fundamental importance for earthquake hazard assessment. Controls on the updip limit were suggested to be related to forearc structure and morphology (Tilmann et al., 2010; Wang & Hu, 2006), metamorphic processes (Moore & Saffer, 2001), or thermal properties (Moore & Saffer, 2001; Oleskevich et al., 1999). Earthquake ruptures that extend into the shallow frontal subduction domain cause larger seafloor displacement and hence trigger potentially large tsunamis as evidenced by a historical slip-to-trench megathrust event offshore Costa Rica (Vannucchi et al., 2017) or exemplified by the 2011 Mw 9.0 Tohoku-Oki earthquake and associated tsunami (Kodaira et al., 2012; Simons et al., 2011). Knowledge of the seismogenic updip limit and its controlling factors are thus essential for assessing subduction zone hazards. Material transfer at subduction zones is primarily governed by either frontal or basal accretion of oceanic sediments or by tectonic erosion at the front and base of the upper plate (hereafter referred to as subduction erosion). A slight majority of subduction zones worldwide are of erosive nature (Scholl & von Huene, 2007; Straub et al., 2020). It has been suggested that subduction erosion and the occurrence of seismicity along subduction zone megathrusts and in the upper overriding plates are inherently related (Wang et al., 2010). Long-term permanent subsidence of the forearc (von Huene & Lallemand, 1990) and the

landward migration of the trench and the volcanic arc (Rutland, 1971) have been linked to subduction erosion (Clift & Vannucchi, 2004). Two modes of subduction erosion have been identified: (1) frontal erosion as commonly caused by the underthrusting of rough seafloor topography, like bending related horst-and-grabens or seamounts colliding with the lower slope (Ranero & von Huene, 2000; Sallarès & Ranero, 2005) and (2) basal erosion by the continuous removal of material from the base of the overriding plate (von Huene et al., 2004) The latter directly impacts the structural development of the plate boundary and might be essential to understand the updip limit of seismic rupture during megathrust earthquakes and the onset of seismicity at the seismogenic updip end (Byrne et al., 1988; Wang et al., 2010). The offshore location of the shallow subduction interface complicates the recording of earthquake-related processes by geophysical data, causing a gap in our understanding of the structural configuration of the plate boundary, overriding plate and subducting plate. Hence, the slip-rate deficit (kinematic coupling ratio) and the detailed seismicity are not accurately resolved during the seismic cycle. However, the extent and termination of coseismic slip are frequently revealed through the spatial distribution of seismicity after the mainshock (Mendoza & Hartzell, 1988), therefore, the postseismic period offers the opportunity to study postseismic processes (Husen et al., 1999; Tilmann et al., 2010).

The South American subduction zone off the coast of northern Chile is a convergent margin dominated by subduction erosion since Mesozoic times (Rutland, 1971; von Huene & Scholl, 1991). This is manifested in the landward migration of the volcanic arc and pervasive extensional faulting of the terrestrial (Allmendinger & González, 2010; Armijo & Thiele, 1990) and marine forearc (Geersen, Ranero, Kopp, et al., 2018; von Huene & Ranero, 2003; von Huene et al., 1999). Further, erosional systems are characterized by the sediment-starved trenches, lacking accretionary prisms and vast amount of trench sediments (Clift & Vannucchi, 2004; Geersen, Ranero, Klauke, et al., 2018). The 2014 Iquique earthquake on 1st April broke a central segment between 19°S and 21°S of the north Chilean seismic gap, which previously ruptured in 1877 during a M~9 earthquake (Figure 1; Comte & Pardo, 1991). A long precursory phase preceded the 2014 mainshock (e.g., Bedford et al., 2015) and devolved into an intense foreshock series before the 2014 Iquique mainshock (Brodsky & Lay, 2014; Cesca et al., 2016; Herman et al., 2016; León-Ríos et al., 2016; Schurr et al., 2014; Yagi et al., 2014). The 2014 Iquique earthquake did not result in enough shallow rupture to trigger a significant tsunami in the Pacific Ocean (An et al., 2014; Lay et al., 2014).

To study the processes that govern the updip limit of seismic rupture in the northern Chilean subduction zone, we combine data from amphibious seismic observations from the postseismic phase of the 2014 Iquique earthquake with multi-channel seismic reflection data of the marine forearc acquired in 2016. We suggest that the updip limit of the 2014 Iquique earthquake activates subduction erosion at the updip limit of the seismogenic zone during the postseismic and possibly the coseismic phase, which leads to extensive faulting of the upper plate, thereby manifesting the location of the updip limit over many earthquake cycles.

2. Data and Methods

We installed two temporary passive seismic networks on the marine forearc. The first deployment was an array of 15 short period ocean bottom seismometers (OBS) 8 months after the April 1, 2014 Iquique mainshock, using the Chilean Navy vessel *OVP Toro*. After 1 year, the seismic network was recovered and 14 OBS were redeployed during *R/V SONNE* cruise SO244/2 in December 2015 and subsequently with a denser station distribution to focus on the updip aftershock distribution (Figure 1). Furthermore, we used waveform data of the permanent seismic network of the Centro Seismológico Nacional (CSN, www.sismologia.cl) and the Integrated Plate Boundary Observatory Chile (IPOC, www.ipoc-network.org).

Earthquakes were detected with the scanloc module of SeisComP3 (GFZ & gempa GmbH, 2008) using a cluster search algorithm to associate phase detections to one or many potential earthquake sources. Source scanning was done with the local 1-D velocity model from Husen et al. (1999). Next, P-phases (Aldersons, 2004; Lange et al., 2012) and S-phases were picked automatically (Diehl et al., 2009), however, automated phase picking on OBS data proved to be unsatisfactory on small magnitude events due to the elevated noise level on some waveform data. Therefore, we manually revised the P- and S-phase onsets of all offshore events.
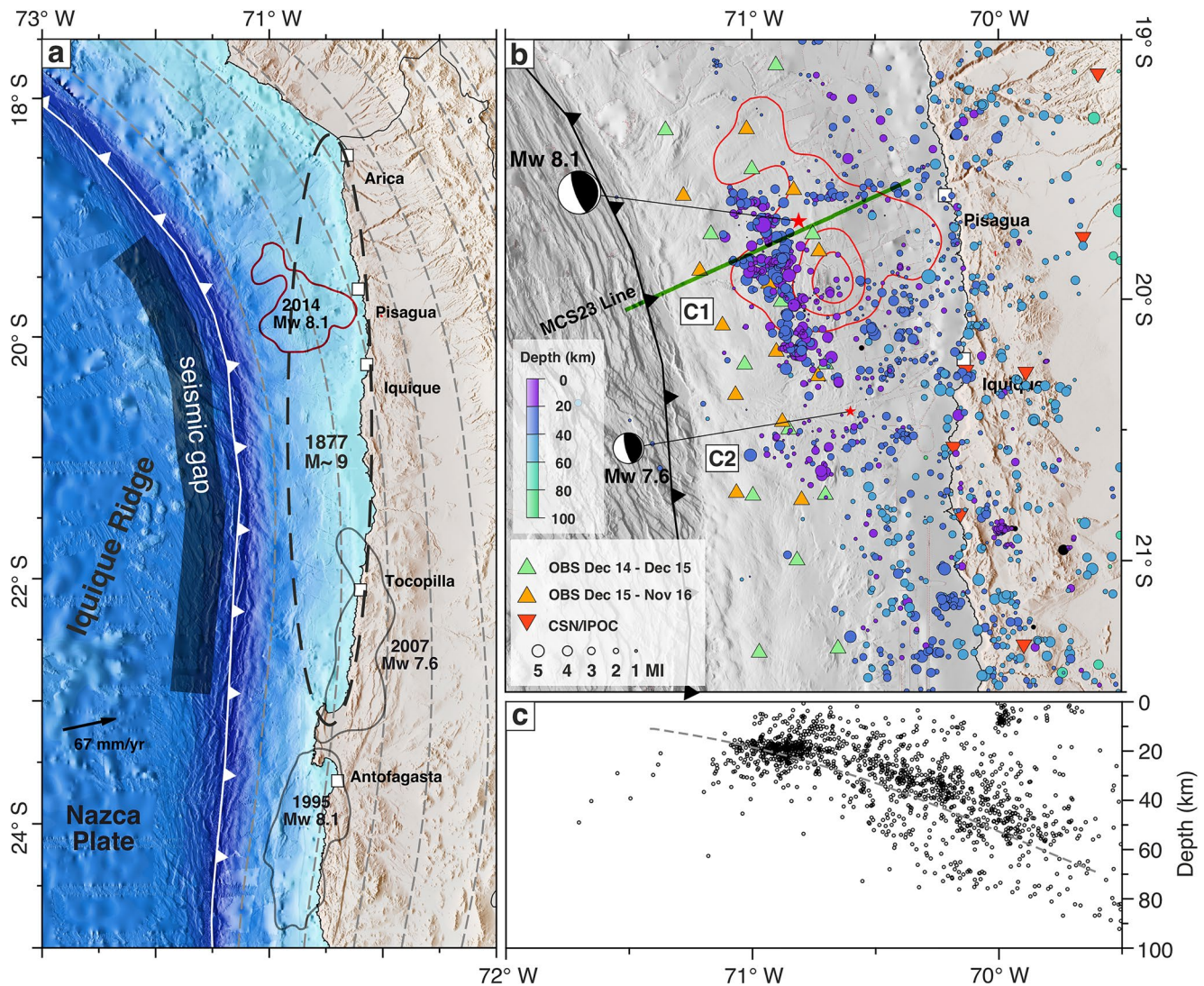
Figure 1. (a) Map of historical earthquakes along northern Chile. The 2014 Iquique earthquake is sketched in red by the 2 m slip contour line (Duputel et al., 2015). The 1,877 M–9 North Chilean earthquake is displayed as an dashed ellipse (Comte & Pardo, 1991), the rupture area of the M8.1 1995 Antofagasta (Chlieh et al., 2004) and the 2007 M7.7 Tocopilla earthquake (Schurr et al., 2012) are outlined by 0.5 m slip contours. Depths of the plate interface (Slab2; Hayes et al., 2018) are shown with dashed gray lines and 20 km depth intervals. Plate convergence rate is shown as a black arrow (Angermann et al., 1999). Bathymetry from Geersen, Ranero, Klauke, et al. (2018) combined with GEBCO, SRTM Topography from Farr et al. (2007). (b) Map of the aftershock hypocenter distribution (1,471 events) of the Mw 8.1 2014 Iquique earthquake from December 9, 2014, until October 31, 2016, recorded by Ocean Bottom Seismometers (OBS) and land stations from the CSN and IPOC networks. C1 marks the updip cluster of the aftershock seismicity and C2 the updip cluster of seismicity following the greatest aftershock with Mw 7.6. The green line indicates the MC23 profile (Tréhu et al., 2017) shown in Figure 2a gCMT solutions indicate the Mw 8.1 2014 Iquique mainshock and the largest M7.6 aftershock. (c) Seismicity cross section of depth versus latitude.

We calculated a minimum 1D velocity model (Husen et al., 1999; Kissling et al., 1995) and a local 2D earthquake tomography for v_p and v_s across the South American margin at 20°S from 71.5°W to 69.4°W using SIMUL2000 (Thurber, 1983, 1992). Subsequently, we estimated absolute locations based on the 2D velocity model with NonLinLoc (Lomax et al., 2000). The velocity model used was constructed from the 2D model transposing it across the whole study region by following the geometry of the trench. Relative hypocenter locations were estimated using a double-difference location scheme (Waldhuser & Ellsworth, 2000). After the final relocation, seismicity in the updip area forms distinct clusters compared to previous processing steps.

Finally, we calculated moment magnitudes (Ottemoller & Havskov, 2003) and local magnitudes (Hutton & Boore, 1987), followed by the calculation of focal mechanisms for 98 stronger events (Reasenberg

et al., 1985). We used focal mechanisms from the Global Centroid Moment Tensor catalog (Dziewonski et al., 1981; Ekström et al., 2012) for the largest events as those overloaded our data loggers, in turn, causing problems in identifying first motion polarities. Additional details on the seismological data processing are given in the supporting information and Figures S1–S12.

To provide additional structural context for the seismicity analysis, we use a multi-channel reflection seismic (MCS) line MC23 acquired during the *R/V Marcus Langseth* cruise MGL1610 in November 2016 (Tréhu et al., 2017). The along-dip MCS profile is processed up to pre-stack depth migration (Ma et al., 2020) and images the structure around the Iquique mainshock down to 35 km depth (Figure 2a). The MCS data were collected with an 8-km long, 640 channel streamer and 6,600 cubic inch airgun array and resolve the plate boundary and the internal structure of the marine forearc in greater detail and to a greater depth than available from previous seismic reflection studies of the northern Chilean margin (Coulbourn & Moberly, 1977; Moberly et al., 1982; von Huene et al., 1999; von Huene & Ranero, 2003; Geersen et al., 2015).

3. Results

3.1. Aftershock Distribution in the Marine Forearc

Our final seismicity catalog spans 23 months and starts eight months after the mainshock occurred (Figure 1). Since we focus on the marine forearc, our local seismic catalog covers the region between 72° W and 69.5°W in longitude and between 22°S and 19°S in latitude, comprising 1,778 local earthquakes (Figure S1). Aftershocks outside this region and deeper than 40 km will be excluded from the following discussion. Generally, the majority of hypocenters are widely distributed, occurring along the plate interface, in the subducting slab, and the overriding plate (Figure 2). However, a significant number of events with higher magnitudes occurred updip of the mainshock and the largest aftershock. These occurred in two major clusters, marked as C1 and C2 in Figure 1, which are separated by a zone of low aftershock activity. C1 forms an NNW-SSE trending band, whereas C2 trends west to east, forming a less focused cluster of smaller magnitude earthquakes. Similar elevated aftershock seismicity updip of the mainshock area has been reported for other subduction zones (e.g., Tilmann et al., 2010) and has elsewhere been correlated to changes in the slope or subducting plate topography interacting with the upper plate (Wang & Bilek, 2014). The elevated Iquique aftershock activity in the shallow marine forearc was previously described in studies using land stations only (León-Ríos et al., 2016; Schurr et al., 2020; Sippl et al., 2018; Soto et al., 2019). However, the seismicity of the marine forearc occurs far outside the land network, resulting in increased uncertainties and a systematic bias in hypocenters for offshore earthquakes. We compare our seismicity with the catalog from Soto et al. (2019). Both catalogs have 23 days and 425 events in common. Soto et al. (2019) observe several west-east striking seismicity streaks interpreted as markers of surrounding aseismic creep along the plate interface. We do not observe the east-west striking seismicity clusters, and offshore our events tend to be located in the continental crust. In general, the horizontal location discrepancies increase with increasing distance from the coast and are largest at the seismogenic updip limit, where the OBS are located (see Figure S8; Soto et al. (2019); Figure S2). We explain the difference between the catalogs by the much better coverage of the forearc seismicity with the OBS stations. Furthermore, we use a more accurate 2D velocity model derived from the offshore seismicity.

The depth uncertainties, estimated by absolute locations, of events in C1, on which the following discussion focusses, shows a range between 0.5 and 2 km (Figure S3) and thus indicates to be a smaller depth error compared to previous seismicity studies offshore Iquique (Sippl et al., 2018; Soto et al., 2019). The observed seismicity in the forearc cross-section of Figure 2 will be described from west to east following the subduction direction. Beneath the outer rise, westward of the trench, no significant seismic activity was detected during the 23 months of OBS recording. Elsewhere outer rise aftershock seismicity has been correlated to slip during large earthquakes that extend to the trench (Sladen & Trevisan, 2018). East of the trench, a ~35 km wide zone with very sparse seismicity is observed. Further East of the observed aseismic zone (>35 km), a large number of events are located within 5 km distance of the plate boundary, that is derived from the multi-channel seismic data. Below the plate interface, seismicity occurred between 20 and 30 km depth, indicating earthquakes are located in the lower plate. Above the plate interface, several earthquakes occurred in the upper plate during the entire observations period. The local earthquake tomography (LET) reveals an elevated v_p/v_s ratio in the upper crust that decreases toward the inner forearc (Figures 2c and
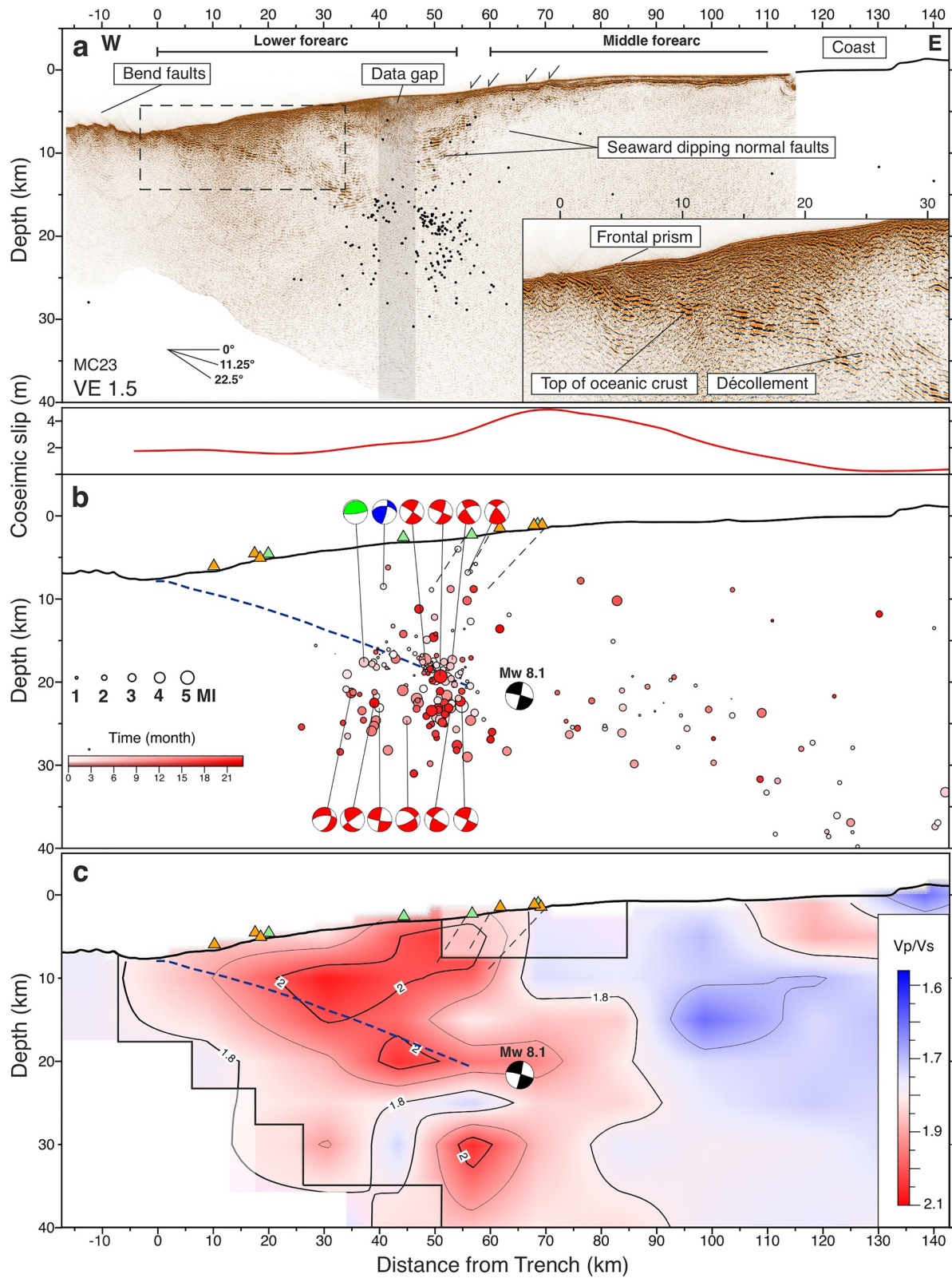
Figure S5). East of the mainshock, the aftershocks are diffusely distributed in the upper crust with local magnitudes mostly lower than 3. The vast majority of focal mechanisms at the seismogenic updip end indicate thrust faulting with one focal plane oriented subparallel to slab dip (Figure S10).

3.2. Marine Forearc Structure and Active Tectonics in the 2014 Iquique Earthquake Region

The multi-channel seismic profile MC23 crosses the epicentral region of the 2014 Iquique earthquake (Figure 1) and images the structure of the incoming and subducting oceanic plate and the marine forearc (Figure 2a). On the incoming plate, the crust of the oceanic Nazca Plate is repeatedly offset by up to 500 m along bending related landward and seaward dipping normal faults (Geersen, Ranero, Klauke, et al., 2018). The trench is characterized by less than 500 m of sediment cover. Landward of the trench, a series of shallow, landward-dipping reflections indicates a ca. 7 km wide frontal prism (Figure 2a). Below the frontal prism, the top of the subducting oceanic basement has a landward dip of ~12°. The high reflectivity of the oceanic basement under the marine forearc can be observed down to depths of ~17 km at 35 km from the trench, where aftershock seismicity commences. Between 50 and 70 km from the trench, a series of pronounced seaward dipping normal faults cut from the seafloor into the framework rock of the upper plate (dashed lines; Figure 2b). Their locations correlate to some of the aftershock hypocenters in the upper plate (also compare Reginato et al., 2020).

4. Discussion

The combined analysis of the 2014 Iquique aftershocks and the seismic reflection image of the marine forearc within the rupture area offers the possibility to link short term deformation associated with a single seismic cycle to the permanent deformation history of an erosive convergent margin. Previous studies of the marine forearc structure of the 2014 Iquique earthquake related the updip aftershock seismicity to postseismic processes, including postseismic relaxation or afterslip (Cesca et al., 2016; León-Ríos et al., 2016; Soto et al., 2019). In contrast to Soto et al. (2019), our aftershock catalog, which is based on 23 months of amphibious and deep crustal MCS data, does not resolve any E-W elongated streaks of seismicity. Instead, we find a broad band of seismicity with individual earthquake clusters updip of the coseismic rupture in the upper and lower plate, besides the plate interface related seismicity. Similar lower plate aftershocks related to the updip limit were observed in Costa Rica (Bilek & Lithgow-Bertelloni, 2005) and Japan (Obana et al., 2013). Obana et al. (2013) related oceanic upper crustal events to bending of the incoming plate since they observed normal faulting events in the oceanic plate. Since we observe few thrust mechanisms at the Iquique updip limit and below the plate interface (in the oceanic plate) this might be similar to thrust faulting in the downgoing plate as observed by Nippress and Rietbrock (2007) after the 1995 Antofagasta earthquake (Figure 1). The thrust faulting in the oceanic crust and mantle was suggested to be associated with the re-activation of horst and graben structures from the plate bending at the outer rise bend (Nippress & Rietbrock, 2007). Above the lower plate seismicity, we document an updip limit of aftershock seismicity that is correlated with crustal reflectivity (Figures 1 and 2b), indicative of long-term along-dip seismo-tectonic segmentation of the subduction zone.

If the updip limit of plate-boundary seismicity is stable in space over many earthquake cycles, it can induce permanent forearc deformation expressed in first-order topographic changes (Rosenau & Oncken, 2009). Indeed, at other subduction zones, similar intense updip clusters of seismicity often correlate with structural or topographic changes of the forearc (Lange et al., 2007; Lieser et al., 2014; Tilmann et al., 2010; Tréhu et al., 2019). Furthermore, such updip seismicity occurs predominantly along the plate boundary. The aftershocks associated with the 2014 Iquique earthquake in northern Chile show a very different pattern. Most

Figure 2. Seismogenic updip limit crossing profile illustrated by different datasets. Subplots A-C showing the same seismicity MCS profile of Figure 1. (a) Pre-stack depth migrated multi-channel seismic reflection line MC23. (b) Coseismic slip from Duputel et al. (2015) above the aftershock distribution (287 events) using a 15 km swath on each side of the seismic profile. The aftershocks are colored according to the time scale from 9th December until the end of the operation in October 2016. Focal mechanisms from FPFIT and gCMT are classified by faulting type in thrust (red), normal (green), strike-slip (yellow), or oblique (blue) fault mechanism. OBS station locations are marked as green and orange triangles. The Mw 8.1 Iquique mainshock hypocenter is indicated by the black focal mechanism. (c) Projection of v_p/v_s ratio from 2D local earthquake tomography to the MCS profile of panel a using the hypocenters from panel (b). Black solid line indicates the region of good resolution.

aftershocks occur in a narrow band roughly updip of the main coseismic rupture (upper panel in Figure 2b), implying postseismic deformation at the seismic-to-aseismic transition. These aftershocks are, however, not associated with a structural or topographic change of the forearc (Figure 2). They are further not limited to the megathrust fault but also occur in the upper overriding and lower subducting plates (Figure 2b).

We interpret the striking aftershock sequence at the updip limit of seismic rupture following the 2014 Iquique earthquake as an indication of active subduction erosion during the coseismic and early postseismic phase. From fossil subduction zones, we have learned that a wide shear zone, as exemplified by the different depths of the 2014 Iquique aftershocks, is characteristic for margins dominated by subduction erosion (Vannucchi et al., 2008). In the concept of subduction erosion, fracturing at the base of the upper plate starts at the updip limit of the seismogenic zone and increases toward the shallow plate interface up to the frontal prism (von Huene et al., 2004). This basal erosion induced by the 2014 Iquique earthquake is indicated by the high number of aftershocks that occur at or slightly above the plate boundary (Figure 2b). Such abrasion of material from the underside of the upper plate is expected to be in a dynamic equilibrium between the removal of material and steepening of forearc slope (von Huene et al., 2004). The associated deformation of the entire upper plate is illustrated by the overall fewer but still significant number of aftershocks above the updip limit of seismic rupture (Figure 2b). These aftershocks seem to occur along seaward dipping planes that match the location of seismically imaged normal faults within the upper plate (Figure 2a). This implies that the faults have moved in the postseismic phase of the 2014 Iquique earthquake. Although the absolute depths of the normal faults are not fully resolved by the seismic data, data from other erosive convergent margins suggest that they may cut to the plate boundary (Contreras-Reyes et al., 2015; Kodaira et al., 2012; Ranero et al., 2008).

While the aftershocks of the 2014 Iquique earthquake represent forearc deformation during the early postseismic phase of one earthquake, the seismically imaged structure of the marine forearc is a result of forearc deformation from hundreds to thousands of seismic cycles (Scholz, 1998). Repeated coseismic and postseismic deformation and associated subduction erosion force extensive faulting and pervasive fracturing at the updip limit of seismic rupture. Deformation is not limited to the plate boundary but active throughout the entire upper plate from the plate boundary to the seafloor (compare Geersen, Ranero, Klauke, et al., 2018). This is consistent with earlier studies based on numerical and analog modeling and conceptional considerations on the relationship between long-term forearc deformation of the overriding plate and earthquake behavior of subduction zone forearcs (Rosenau & Oncken, 2009; Wang & Hu, 2006). Northern Chile is an end-member margin in terms of trench sediment thickness, and subduction erosion is likely the dominant tectonic mode since at least Mesozoic times (Rutland, 1971). This is manifested in about 250 km loss of overriding continental plate since 150 Ma (Scheuber & Reutter, 1992) and associated eastward migration of the trench and volcanic arc. Over time, tectonic erosion of the upper plate (von Huene & Ranero, 2003) causes the updip limit to migrate landwards, mimicking the migration of the volcanic arc and the trench.

In the Iquique region of the 2014 Iquique earthquake, long-term upper plate faulting and fracturing at the updip limit of the seismogenic zone are manifested in the permanent deformation pattern of the marine forearc seaward of the 2014 Iquique aftershocks. This part of the marine forearc between the trench and the current updip limit (40 km distance) has migrated through the updip limit over the last millions of years. It is heavily faulted as indicated by discontinuous seismic reflections. The overall high reflection amplitudes in this region further support a high degree of fracturing and possibly fluids within the fractures. The elevated v_p/v_s ratio in the upper plate recognized from local earthquake tomography (Figure 2c) further supports the presence of fluids in the highly fractured outermost marine forearc (Popp & Kern, 1994; Wang et al., 2012). The fractured and fluid-rich outermost marine forearc, seaward of the 2014 Iquique earthquake rupture is likely too weak (and heavily deformed) to store sufficient elastic energy to nucleate a great earthquake. Further down-dip, the decrease in faulting and fluid content in the marine forearc, together with the onset of aftershock seismicity, indicates an increase in strength of the overriding plate that allows the storing of elastic energy (Figure 3). A similar down-dip segmentation of the North Chilean forearc that can build up elastic energy and rupture during great earthquakes has been previously suggested based on gravity data and seismic velocity structure (Contreras-Reyes et al., 2012; Maksymowicz et al., 2018; Sallarès & Ranero, 2005). The segmentation is in-line with our amphibious aftershock observation of the 2014 Iquique earthquake rupture. It is further supported by the decrease of coseismic rupture at the transition from the
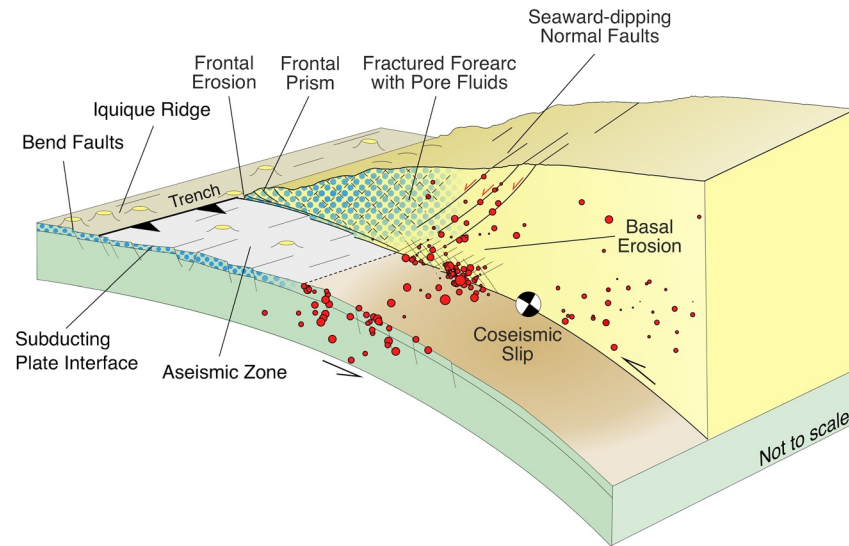
Figure 3. Conceptional model of seismotectonic segmentation and basal erosion of the North Chilean margin offshore Iquique. Pore-fluid extent marks the region of increased v_p/v_s ratio.

heavily deformed outermost marine forearc to the less deformed section of the forearc between the coast and the updip limit of the seismic rupture (Duputel et al., 2015; Jara et al., 2018; Schurr et al., 2014).

5. Conclusions

Combining 2 years of local seismicity observations following the 2014 Iquique earthquake and structural constraints on forearc architecture derived from MCS data, we provide evidence for the interplay of plate boundary rupture and upper plate deformation in the context of long-term subduction erosion. The majority of aftershocks of the 2014 Iquique earthquake occurred updip of the coseismic slip and ~32–60 km landward of the trench. Although most of the seismicity was within ~5 km of the plate boundary, earthquakes extended through the upper plate, defining a seaward dipping zone that coincides with seaward dipping normal faults imaged in the MCS data. The updip band of aftershock seismicity separates a pervasively fractured and likely fluid-filled marine forearc farther seaward from a less deformed section of the upper plate forearc. At the transition, active subduction erosion during the postseismic and possibly coseismic phases leads to basal abrasion of the upper plate and associated extensional faulting of the upper plate at the updip end of the seismogenic zone. Landward migration of the updip end of the seismogenic zone, at similar rates compared to the trench and the volcanic arc, preconditions the structural setting of the heavily fractured, fluid-filled and therefore weak and aseismic outermost marine forearc.

Data Availability Statement

The seismic waveform data from network CX are available from GFZ and CNRS-INSU (2006). OBS seismic catalog and waveform data are available from PANGAEA https://doi.pangaea.de/10.1594/PANGAEA.929899. Arrival times from the permanent land network were provided by the CSN (Barrientos, 2018). Earthquake focal mechanisms were obtained from Global Centroid-Moment-Tensor catalog (https://www.globalcmt.org/). Multibeam data from Geersen, Ranero, Klauke, et al., (2018) can be accessed via https://doi.pangaea.de/10.1594/PANGAEA.893034.

References

Aldersons, F. (2004). *Toward a three-dimensional crustal structure of the dead sea region from local earthquake tomography. (Ph.D. thesis).* Israel: Tel-Aviv University.

Allmendinger, R. W., & González, G. (2010). Invited review paper: Neogene to Quaternary tectonics of the coastal Cordillera, northern Chile. *Tectonophysics*, *495*(1–2), 93–110. https://doi.org/10.1016/j.tecto.2009.04.019

An, C., Sepúlveda, I., & Liu, P. L.-F. (2014). Tsunami source and its validation of the 2014 Iquique, Chile, earthquake. *Geophysical Research Letters*, *41*(11), 3988–3994. https://doi.org/10.1002/2014gl060567

Angermann, D., Klotz, J., & Reigber, C. (1999). Space-geodetic estimation of the nazca-south america euler vector. *Earth and Planetary Science Letters*, *171*(3), 329–334. https://doi.org/10.1016/s0012-821x(99)00173-9

Armijo, R., & Thiele, R. (1990). Active faulting in northern Chile: Ramp stacking and lateral decoupling along a subduction plate boundary? *Earth and Planetary Science Letters*, *98*(1), 40–61. https://doi.org/10.1016/0012-821x(90)90087-e

Barrientos, S. (2018). The Seismic Network of Chile. *Seismological Research Letters*, *89*(2A), 467–474. https://doi.org/10.1785/0220160195

Bedford, J., Moreno, M., Schurr, B., Bartsch, M., & Oncken, O. (2015). Investigating the final seismic swarm before the Iquique-Pisagua 2014 M w 8.1 by comparison of continuous GPS and seismic foreshock data. *Geophysical Research Letters*, *42*(10), 3820–3828. https://doi.org/10.1002/2015gl063953

Bilek, S. L., & Lithgow-Bertelloni, C. (2005). Stress changes in the Costa Rica subduction zone due to the 1999 Mw=6.9 Quepos earthquake. *Earth and Planetary Science Letters*, *230*(1–2), 97–112. https://doi.org/10.1016/j.epsl.2004.11.020

Brodsky, E. E., & Lay, T. (2014). Recognizing foreshocks from the 1 April 2014 Chile earthquake. *Science*, *344*(6185), 700–702. https://doi.org/10.1126/science.1255202

Byrne, D. E., Davis, D. M., & Sykes, L. R. (1988). Loci and maximum size of thrust earthquakes and the mechanics of the shallow region of subduction zones. *Tectonics*, *7*(4), 833–857. https://doi.org/10.1029/TC007i004p00833

Cesca, S., Grigoli, F., Heimann, S., Dahm, T., Kriegerowski, M., Sobiesiak, M., et al. (2016). The Mw8.1 2014 Iquique, Chile, seismic sequence: A tale of foreshocks and aftershocks. *Geophysical Journal International*, *204*(3), 1766–1780. https://doi.org/10.1093/gji/ggv544

Chlieh, M., de Chabalier, J. B., Ruegg, J. C., Armijo, R., Dmowska, R., Campos, J., & Feigl, K. L. (2004). Crustal deformation and fault slip during the seismic cycle in the North Chile subduction zone, from GPS and InSAR observations. *Geophysical Journal International*, *158*(2), 695–711. https://doi.org/10.1111/j.1365-246X.2004.02326.x

Clift, P., & Vannucchi, P. (2004). Controls on tectonic accretion versus erosion in subduction zones: Implications for the origin and recycling of the continental crust. *Reviews of Geophysics*, *42*(2). https://doi.org/10.1029/2003rg000127

Comte, D., & Pardo, M. (1991). Reappraisal of great historical earthquakes in the northern Chile and southern Peru seismic gaps. *Natural Hazards*, *4*(1), 23–44. https://doi.org/10.1007/bf00126557

Contreras-Reyes, E., Jara, J., Grevemeyer, I., Ruiz, S., & Carrizo, D. (2012). Abrupt change in the dip of the subducting plate beneath north Chile. *Nature Geoscience*, *5*(5), 342–345. https://doi.org/10.1038/ngeo1447

Contreras-Reyes, E., Ruiz, J. A., Becerra, J., Kopp, H., Reichert, C., Maksymowicz, A., & Arriagada, C. (2015). Structure and tectonics of the central Chilean margin (31°-33°S): Implications for subduction erosion and shallow crustal seismicity. *Geophysical Journal International*, *203*(2), 776–791. https://doi.org/10.1093/gji/ggv309

Coulbourn, W. T., & Moberly, R. (1977). Structural evidence of the evolution of fore-arc basins off South America. *Canadian Journal of Earth Sciences*, *14*(1), 102–116. https://doi.org/10.1139/e77-011

Diehl, T., Deichmann, N., Kissling, E., & Husen, S. (2009). Automatic S-Wave picker for local earthquake tomography. *Bulletin of the Seismological Society of America*, *99*(3), 1906–1920. https://doi.org/10.1785/0120080019

Duputel, Z., Jiang, J., Jolivet, R., Simons, M., Rivera, L., Ampuero, J. P., et al. (2015). The Iquique earthquake sequence of April 2014: Bayesian modeling accounting for prediction uncertainty. *Geophysical Research Letters*, *42*(19), 7949–7957. https://doi.org/10.1002/2015gl065402

Dziewonski, A. M., Chou, T.-A., & Woodhouse, J. H. (1981). Determination of earthquake source parameters from waveform data for studies of global and regional seismicity. *Journal of Geophysical Research*, *86*(B4), 2825–2852. https://doi.org/10.1029/JB086iB04p02825

Ekström, G., Nettles, M., & Dziewoński, A. M. (2012). The global CMT project 2004-2010: Centroid-moment tensors for 13,017 earthquakes. *Physics of the Earth and Planetary Interiors*, *200–201*, 1–9. https://doi.org/10.1016/j.pepi.2012.04.002

Farr, T. G., Rosen, P. A., Caro, E., Crippen, R., Duren, R., Hensley, S., et al. (2007). The shuttle radar topography mission. *Reviews of Geophysics*, *45*(2). https://doi.org/10.1029/2005rg000183

Geersen, J., Ranero, C. R., Barckhausen, U., & Reichert, C. (2015). Subducting seamounts control interplate coupling and seismic rupture in the 2014 Iquique earthquake area. *Nature Communications*, *6*, 8267. https://doi.org/10.1038/ncomms9267

Geersen, J., Ranero, C. R., Klaucke, I., Behrmann, J. H., Kopp, H., Tréhu, A. M., et al. (2018a). Active tectonics of the North Chilean marine forearc and adjacent oceanic Nazca Plate. *Tectonics*, *37*(11), 4194–4211. https://doi.org/10.1029/2018tc005087

Geersen, J., Ranero, C. R., Kopp, H., Behrmann, J. H., Lange, D., Klaucke, I., et al. (2018b). Does permanent extensional deformation in lower forearc slopes indicate shallow plate-boundary rupture? *Earth and Planetary Science Letters*, *489*, 17–27. https://doi.org/10.1016/j.epsl.2018.02.030

GFZ & CNRS-INSU. (2006). IPOC seismic network. Integrated plate boundary observatory Chile - IPOC. Other/Seismic Network. https://doi.org/10.14470/PK615318

GFZ & gempa GmbH. (2008). *The SeisComP seismological software package*. GFZ Data Services. https://doi.org/10.5880/GFZ.2.4.2020.003

Hayes, G. P., Moore, G. L., Portner, D. E., Hearne, M., Flamme, H., Furtney, M., & Smoczyk, G. M. (2018). Slab2, A comprehensive subduction zone geometry model. *Science*, *362*(6410), 58–61. https://doi.org/10.1126/science.aat4723

Herman, M. W., Furlong, K. P., Hayes, G. P., & Benz, H. M. (2016). Foreshock triggering of the 1 April 2014 Mw 8.2 Iquique, Chile, earthquake. *Earth and Planetary Science Letters*, *447*, 119–129. https://doi.org/10.1016/j.epsl.2016.04.020

Husen, S., Kissling, E., Flueh, E. R., & Asch, G. (1999). Accurate hypocenter determination in the seismogenic zone of the subducting Nazca Plate in northern Chile using a combined on-/offshore network. *Geophysical Journal International*, *138*(3), 687–701. https://doi.org/10.1046/j.1365-246x.1999.00893.x

Hutton, L. K., & Boore, D. M. (1987). The ML scale in Southern California. *Bulletin of the Seismological Society of America*, *77*(6), 2074–2094.

Jara, J., Sánchez-Reyes, H., Socquet, A., Cotton, F., Virieux, J., Maksymowicz, A., et al. (2018). Kinematic study of Iquique 2014 M 8.1 earthquake: Understanding the segmentation of the seismogenic zone. *Earth and Planetary Science Letters*, *503*, 131–143. https://doi.org/10.1016/j.epsl.2018.09.025

Kissling, E., Kradolfer, U., & Maurer, H. (1995). *Program VELEST user's guide-short introduction*. Institute of Geophysics, ETH Zuerich.

Kodaira, S., No, T., Nakamura, Y., Fujiwara, T., Kaiho, Y., Miura, S., et al. (2012). Coseismic fault rupture at the trench axis during the 2011 Tohoku-oki earthquake. *Nature Geoscience*, *5*(9), 646–650. https://doi.org/10.1038/ngeo1547

Lange, D., Rietbrock, A., Haberland, C., Bataille, K., Dahm, T., Tilmann, F., & Flüh, E. R. (2007). Seismicity and geometry of the south Chilean subduction zone (41.5°S-43.5°S): Implications for controlling parameters. *Geophysical Research Letters*, *34*(6). https://doi.org/10.1029/2006gl029190

Lange, D., Tilmann, F., Barrientos, S. E., Contreras-Reyes, E., Methe, P., Moreno, M., et al. (2012). Aftershock seismicity of the 27 February 2010 Mw 8.8 Maule earthquake rupture zone. *Earth and Planetary Science Letters*, *317–318*, 413–425. https://doi.org/10.1016/j.epsl.2011.11.034

Lay, T., Yue, H., Brodsky, E. E., & An, C. (2014). The April 1, 2014 Iquique, Chile, Mw 8.1 earthquake rupture sequence. *Geophysical Research Letters*, *41*(11), 3818–3825. https://doi.org/10.1002/2014gl060238

León-Ríos, S., Ruiz, S., Maksymowicz, A., Leyton, F., Fuenzalida, A., & Madariaga, R. (2016). Diversity of the 2014 Iquique's foreshocks and aftershocks: Clues about the complex rupture process of a Mw 8.1 earthquake. *Journal of Seismology*, *20*(4), 1059–1073. https://doi.org/10.1007/s10950-016-9568-6

Lieser, K., Grevemeyer, I., Lange, D., Flueh, E., Tilmann, F., & Contreras-Reyes, E. (2014). Splay fault activity revealed by aftershocks of the 2010 Mw 8.8 Maule earthquake, central Chile. *Geology*, *42*(9), 823–826. https://doi.org/10.1130/g35848.1

Lomax, A., Virieux, J., Volant, P., & Berge-Thierry, C. (2000). Probabilistic Earthquake Location in 3D and Layered Models. *Advances in seismic event location* (Vol. *18*, pp. 101–134).

Ma, B., Klaeschen, D., Kopp, H., Geersen, J., & Tréhu, A. M. (2020). *Variations in plate interface reflectivity within the rupture zone of the 2014 Iquique earthquake sequence: Evidence from seismic and bathymetric data*. AGU Fall Meeting 2020. https://agu.confex.com/agu/fm20/meetingapp.cgi/Paper/680334

Maksymowicz, A., Ruiz, J., Vera, E., Contreras-Reyes, E., Ruiz, S., Arraigada, C., et al. (2018). Heterogeneous structure of the Northern Chile marine forearc and its implications for megathrust earthquakes. *Geophysical Journal International*, *215*(2), 1080–1097. https://doi.org/10.1093/gji/ggy325

Mendoza, C., & Hartzell, S. (1988). Aftershock patterns and main shock faulting. *Bulletin of the Seismological Society of America*, *78*(4), 1438–1449.

Moberly, R., Shepherd, G. L., & Coulbourn, W. T. (1982). Forearc and other basins, continental margin of northern and southern Peru and adjacent Ecuador and Chile. *Geological Society, London, Special Publications*, *10*(1), 171–189. https://doi.org/10.1144/gsl.Sp.1982.010.01.11

Moore, J. C., & Saffer, D. (2001). Updip limit of the seismogenic zone beneath the accretionary prism of southwest Japan: An effect of diagenetic to low-grade metamorphic processes and increasing effective stress. *Geologica*, *29*(2), 183–186. https://doi.org/10.1130/0091-7613(2001)029<0183:Ulotsz>2.0.Co;2

Nippress, S. E. J., & Rietbrock, A. (2007). Seismogenic zone high permeability in the Central Andes inferred from relocations of micro-earthquakes. *Earth and Planetary Science Letters*, *263*(3–4), 235–245. https://doi.org/10.1016/j.epsl.2007.08.032

Obana, K., Kodaira, S., Shinohara, M., Hino, R., Uehira, K., Shiobara, H., et al. (2013). Aftershocks near the updip end of the 2011 Tohoku-Oki earthquake. *Earth and Planetary Science Letters*, *382*, 111–116. https://doi.org/10.1016/j.epsl.2013.09.007

Oleskevich, D. A., Hyndman, R. D., & Wang, K. (1999). The updip and downdip limits to great subduction earthquakes: Thermal and structural models of Cascadia, south AK, SW Japan, and Chile. *Journal of Geophysical Research*, *104*(B7), 14965–14991. https://doi.org/10.1029/1999jb900060

Ottemoller, L., & Havskov, J. (2003). Moment magnitude determination for local and regional earthquakes based on source spectra. *Bulletin of the Seismological Society of America*, *93*(1), 203–214. https://doi.org/10.1785/0120010220

Popp, T., & Kern, H. (1994). The influence of dry and water saturated cracks on seismic velocities of crustal rocks - A comparison of experimental data with theoretical model. *Surveys in Geophysics*, *15*(5), 443–465. https://doi.org/10.1007/bf00690169

Ranero, C. R., Grevemeyer, I., Sahling, H., Barckhausen, U., Hensen, C., Wallmann, K., et al. (2008). Hydrogeological system of erosional convergent margins and its influence on tectonics and interplate seismogenesis. *Geochemistry, Geophysics, Geosystems*, *9*(3). https://doi.org/10.1029/2007gc001679

Ranero, C. R., & von Huene, R. (2000). Subduction erosion along the Middle America convergent margin. *Nature*, *404*(6779), 748–752. https://doi.org/10.1038/35008046

Reasenberg, P., Oppenheimer, D., & USGS. (1985). FPFIT, FPPLOT and FPPAGE Fortran computer programs for calculating and displaying earthquake fault-plane solutions. *U.S. Geological Survey Open-File Report*, 85–739.

Reginato, G., Vera, E., Contreras-Reyes, E., Tréhu, A. M., Maksymowicz, A., Bello-González, J. P., & González, F. (2020). Seismic structure and tectonics of the continental wedge overlying the source region of the Iquique Mw 8.1 2014 earthquake. *Tectonophysics*, *796*, 228629. https://doi.org/10.1016/j.tecto.2020.228629

Rosenau, M., & Oncken, O. (2009). Fore-arc deformation controls frequency-size distribution of megathrust earthquakes in subduction zones. *Journal of Geophysical Research*, *114*(B10). https://doi.org/10.1029/2009jb006359

Rutland, R. W. R. (1971). Andean orogeny and ocean floor spreading. *Nature*, *233*(5317), 252–255. https://doi.org/10.1038/233252a0

Sallarès, V., & Ranero, C. (2005). Structure and tectonics of the erosional convergent margin off Antofagasta, north Chile (23°30′S). *Journal of Geophysical Research*, *110*(B6). https://doi.org/10.1029/2004jb003418

Scheuber, E., & Reutter, K.-J. (1992). Magmatic arc tectonics in the Central Andes between 21° and 25°S. *Tectonophysics*, *205*(1–3), 127–140. https://doi.org/10.1016/0040-1951(92)90422-3

Scholl, D., & von Huene, R. (2007). Crustal recycling at modern subduction zones applied to the past—Issues of growth and preservation of continental basement crust, mantle geochemistry, and supercontinent reconstruction. In R. D. J. Hatcher, M. P. Carlson, J. H. McBride, & J. R. M. Catalán (Eds.), *4-D framework of continental crust*. Geological Society of America.

Scholz, C. H. (1998). Earthquakes and friction laws. *Nature*, *391*, 37–42. https://doi.org/10.1038/34097

Schurr, B., Asch, G., Hainzl, S., Bedford, J., Hoechner, A., Palo, M., et al. (2014). Gradual unlocking of plate boundary controlled initiation of the 2014 Iquique earthquake. *Nature*, *512*(7514), 299–302. https://doi.org/10.1038/nature13681

Schurr, B., Asch, G., Rosenau, M., Wang, R., Oncken, O., Barrientos, S., et al. (2012). The 2007 M7.7 Tocopilla northern Chile earthquake sequence: Implications for along-strike and downdip rupture segmentation and megathrust frictional behavior. *Journal of Geophysical Research*, *117*(B5). https://doi.org/10.1029/2011jb009030

Schurr, B., Moreno, M., Tréhu, A. M., Bedford, J., Kummerow, J., Li, S., & Oncken, O. (2020). Forming a mogi doughnut in the years prior to and immediately before the 2014 M 8.1 Iquique, Northern Chile, Earthquake. *Geophysical Research Letters*, *47*(16). https://doi.org/10.1029/2020gl088351

Simons, M., Minson, S. E., Sladen, A., Ortega, F., Jiang, J., Owen, S. E., et al. (2011). The 2011 magnitude 9.0 Tohoku-Oki earthquake: Mosaicking the megathrust from seconds to centuries. *Science*, *332*(6036), 1421–1425. https://doi.org/10.1126/science.1206731

Sippl, C., Schurr, B., Asch, G., & Kummerow, J. (2018). Seismicity structure of the Northern Chile forearc from >100,000 double-difference relocated hypocenters. *Journal of Geophysical Research Solid Earth*, *123*(5), 4063–4087. https://doi.org/10.1002/2017jb015384

Sladen, A., & Trevisan, J. (2018). Shallow megathrust earthquake ruptures betrayed by their outer-trench aftershocks signature. *Earth and Planetary Science Letters*, *483*, 105–113. https://doi.org/10.1016/j.epsl.2017.12.006

Soto, H., Sippl, C., Schurr, B., Kummerow, J., Asch, G., Tilmann, F., et al. (2019). Probing the Northern Chile megathrust with seismicity: The 2014 M8.1 Iquique Earthquake sequence. *Journal of Geophysical Research Solid Earth*, *124*(12), 12935–12954. https://doi.org/10.1029/2019jb017794

Straub, S. M., Gómez-Tuena, A., & Vannucchi, P. (2020). Subduction erosion and arc volcanism. *Nature Reviews Earth Environment*, *1*(11), 574–589. https://doi.org/10.1038/s43017-020-0095-1

Thurber, C. H. (1983). Earthquake locations and three-dimensional crustal structure in the Coyote Lake Area, central California. *Journal of Geophysical Research*, *88*(B10), 8226. https://doi.org/10.1029/JB088iB10p08226

Thurber, C. H. (1992). Hypocenter-velocity structure coupling in local earthquake tomography. *Physics of the Earth and Planetary Interiors*, *75*(1–3), 55–62. https://doi.org/10.1016/0031-9201(92)90117-e

Tilmann, F. J., Craig, T. J., Grevemeyer, I., Suwargadi, B., Kopp, H., & Flueh, E. (2010). The updip seismic/aseismic transition of the Sumatra megathrust illuminated by aftershocks of the 2004 Aceh-Andaman and 2005 Nias events. *Geophysical Journal International*, *181*(3), 1261–1274. https://doi.org/10.1111/j.1365-246X.2010.04597.x

Tréhu, A. M., Hass, B., de Moor, A., Maksymowicz, A., Contreras-Reyes, E., Vera, E., & Tryon, M. D. (2019). Geologic controls on up-dip and along-strike propagation of slip during subduction zone earthquakes from a high-resolution seismic reflection survey across the northern limit of slip during the 2010 Mw 8.8 Maule earthquake, offshore Chile. *Geosphere*, *15*(6), 1751–1773. https://doi.org/10.1130/ges02099.1

Tréhu, A. M., Vera, E., & Riedel, M. (2017). PICTURES: Pisagua/Iquique crustal tomography to understand the region of the earthquake source. *MGL1610 Cruise Report*.

Vannucchi, P., Remitti, F., & Bettelli, G. (2008). Geological record of fluid flow and seismogenesis along an erosive subducting plate boundary. *Nature*, *451*(7179), 699–703. https://doi.org/10.1038/nature06486

Vannucchi, P., Spagnuolo, E., Aretusini, S., Di Toro, G., Ujiie, K., Tsutsumi, A., & Nielsen, S. (2017). Past seismic slip-to-the-trench recorded in Central America megathrust. *Nature Geoscience*, *10*(12), 935–940. https://doi.org/10.1038/s41561-017-0013-4

von Huene, R., & Lallemand, S. (1990). Tectonic erosion along the Japan and Peru convergent margins. *Geological Society of America Bulletin*, *102*(6), 704–720. https://doi.org/10.1130/0016-7606(1990)102<0704:TEATJA>2.3.CO;2

von Huene, R., & Ranero, C. R. (2003). Subduction erosion and basal friction along the sediment-starved convergent margin off Antofagasta, Chile. *Journal of Geophysical Research*, *108*(B2). https://doi.org/10.1029/2001jb001569

von Huene, R., Ranero, C. R., & Vannucchi, P. (2004). Generic model of subduction erosion. *Geologica*, *32*(10), 913. https://doi.org/10.1130/g20563.1

von Huene, R., & Scholl, D. W. (1991). Observations at convergent margins concerning sediment subduction, subduction erosion, and the growth of continental crust. *Reviews of Geophysics*, *29*(3), 279. https://doi.org/10.1029/91rg00969

von Huene, R., Weinrebe, W., & Heeren, F. (1999). Subduction erosion along the North Chile margin. *Journal of Geodynamics*, *27*(3), 345–358. https://doi.org/10.1016/s0264-3707(98)00002-7

Waldhuser, F., & Ellsworth, W. L. (2000). A Double-difference Earthquake location algorithm Method and application to the Northern Hayward Fault, California. *Bulletin of the Seismological Society of America*, *90*(6), 1253–1368. https://doi.org/10.1785/0120000006

Wang, K., & Bilek, S. L. (2014). Invited review paper: Fault creep caused by subduction of rough seafloor relief. *Tectonophysics*, *610*, 1–24. https://doi.org/10.1016/j.tecto.2013.11.024

Wang, K., & Hu, Y. (2006). Accretionary prisms in subduction earthquake cycles: The theory of dynamic Coulomb wedge. *Journal of Geophysical Research*, *111*(B6). https://doi.org/10.1029/2005jb004094

Wang, K., Hu, Y., von Huene, R., & Kukowski, N. (2010). Interplate earthquakes as a driver of shallow subduction erosion. *Geology*, *38*(5), 431–434. https://doi.org/10.1130/g30597.1

Wang, X.-Q., Schubnel, A., Fortin, J., David, E. C., Guéguen, Y., & Ge, H.-K. (2012). High Vp/Vs ratio: Saturated cracks or anisotropy effects? *Geophysical Research Letters*, *39*(L11307). https://doi.org/10.1029/2012GL051742

Wessel, P., Smith, W. H. F., Scharroo, R., Luis, J., & Wobbe, F. (2013). Generic mapping tools: Improved version released. *Eos Transaction American Geophysical Union*, *94*(45), 409–410. https://doi.org/10.1002/2013eo450001

Yagi, Y., Okuwaki, R., Enescu, B., Hirano, S., Yamagami, Y., Endo, S., & Komoro, T. (2014). Rupture process of the 2014 Iquique Chile Earthquake in relation with the foreshock activity. *Geophysical Research Letters*, *41*(12), 4201–4206. https://doi.org/10.1002/2014GL060274

References from the Supporting Information

Collings, R., Lange, D., Rietbrock, A., Tilmann, F., Natawidjaja, D., Suwargadi, B., et al. (2012). Structure and seismogenic properties of the Mentawai segment of the Sumatra subduction zone revealed by local earthquake traveltime tomography. *Journal of Geophysical Research*, *117*(B1). https://doi.org/10.1029/2011jb008469

Haberland, C., Rietbrock, A., Lange, D., Bataille, K., & Dahm, T. (2009). Structure of the seismogenic zone of the southcentral Chilean margin revealed by local earthquake traveltime tomography. *Journal of Geophysical Research*, *114*(B1). https://doi.org/10.1029/2008jb005802

Havskov, J., Voss, P. H., & Ottemöller, L. (2020). Seismological Observatory Software: 30 Yr of SEISAN. *Seismological Research Letters*, *91*(3), 1846–1852. https://doi.org/10.1785/0220190313

Husen, S., & Smith, R. B. (2004). Probabilistic Earthquake Relocation in Three-Dimensional Velocity Models for the Yellowstone National Park Region, Wyoming. *Bulletin of the Seismological Society of America*, *94*(3), 880–896. https://doi.org/10.1785/0120030170

Sielfeld, G., Lange, D., & Cembrano, J. (2019). Intra-Arc Crustal seismicity: Seismotectonic implications for the Southern Andes Volcanic Zone, Chile. *Tectonics*, *38*(2), 552–578. https://doi.org/10.1029/2018tc004985